International Journal of Architectural, Civil and Construction Sciences
ISSN: 2415-1734
Vol:10, No:6, 2016

Response of a Bridge Crane during an Earthquake

F. Fekak, A. Gravouil, M. Brun, B. Depale

***Abstract*—**During an earthquake, a bridge crane may be subjected to multiple impacts between crane wheels and rail. In order to model such phenomena, a time-history dynamic analysis with a multi-scale approach is performed. The high frequency aspect of the impacts between wheels and rails is taken into account by a Lagrange explicit event-capturing algorithm based on a velocity-impulse formulation to resolve contacts and impacts. An implicit temporal scheme is used for the rest of the structure. The numerical coupling between the implicit and the explicit schemes is achieved with a heterogeneous asynchronous time-integrator.

***Keywords*—**Earthquake, bridge crane, heterogeneous asynchronous time-integrator, impacts.

I. Introduction

HOISTING appliances such as bridge cranes are heavy mobile systems. They are located overhead in buildings or warehouses.

Usual computational methods of such equipment, subjected to an earthquake, are based on a modal representation of the structures using spectral responses. This method assumes geometric linearity (small deformations and small displacements), material linearity (elastic materials) and a linear behavior at the interfaces (no impacts). Consequently, this can lead to an overestimate of seismic loads used to design a bridge crane. In order to avoid this, it becomes necessary to use sophisticated methods in which the vertical and horizontal impacts between crane wheels and rails are introduced. The qualification of these structures with respect to normative seismic design requirements, which are continuously developing, requires strengthened simulation techniques if an overestimation loads used to design this equipment is to be avoid. Consequently, the use of time-history analysis, based on ground accelerograms, has become more usual.

This paper led by Cetim (the Technical Center for the Mechanical Industry) and LaMCos (Contact and Structure Mechanics Laboratory) is aimed at more accurate modelling of the behavior of a bridge crane subjected to multiple impacts.

The first part of this work consists of the development of an explicit event-capturing impact algorithm based on a velocity-impulse formulation. In the second part of this work, a heterogeneous asynchronous time-integrator is applied to a bridge crane subjected to a temporal acceleration.

F. Fekak and B. Depale are with the Technical center for the mechanical industry, 52, avenue Felix Louat, 60300, Senlis, France (phone: +33-344-673-444; e-mail: {Bruno.depale, fatima-ezzahra.fekak}@cetim.fr).

A. Gravouil is with Université de Lyon, INSA de Lyon, LaMCoS, CNRS UMR 5259, 18-20, rue des Sciences, F-69621, Villeurbanne, France (e-mail: anthony.gravouil@insa-lyon.fr).

M. Brun is with Université de Lyon, INSA-Lyon, LGCIE, EA 4126, 34, rue des Arts, F-69621, Villeurbanne, France (e-mail: michael.brun@insa-lyon.fr).

II. Dynamic Contact and Impact Modelling

A. Local Velocity-Impulse Formulation

We consider a unilateral contact without friction between two bodies Ω_1 (wheel) and Ω_2 (rail). Γ_C is the contact surface. The unilateral contact formulation, expressed in terms of velocity and impulse, is written at the contact surface Γ_C as [1], [2]:

$$\begin{cases} \dot{g}_N = (\mathbf{v}_1 - \mathbf{v}_2).\mathbf{n}_1 \geq 0 \\ i_N^\alpha = \boldsymbol{\sigma}_\alpha.\mathbf{n}_\alpha.\mathbf{n}_\alpha \leq 0;\ \alpha = 1 \text{ or } 2 \\ \dot{g}_N.i_N^\alpha = 0 \end{cases} \quad (1)$$

where $\boldsymbol{n}_\alpha$ is the external normal to the contact surface Γ_C, $\boldsymbol{\sigma}_\alpha$ represents the Cauchy stress tensor existing in Ω_α, $\dot{g}_N$ is the normal component of the relative velocity, i_N^α is the contact impulse in Ω_α.

The first inequality of (1) represents the non-penetration condition of two solids in contact. The second inequality shows that perpendicular loads due to contact can only be compressive. The third equation, also called complementarity condition, reflects that in any time point there is either contact ($\dot{g}_N = 0$), or rebound ($i_N^\alpha = 0$).

B. Lagrange Explicit Contact/Impact Algorithm

The enforcement of unilateral contact constraints may generate impacts which introduce time discontinuities (velocity jumps) in the balance equations. This non-smoothness requests the development of specific time-integrators.

Based on the Lagrange multipliers method, the non-smooth semi-discrete form of a contact/impact problem can be summarized as [2]:

$$\begin{cases} \mathbf{M}\mathrm{d}\dot{\mathbf{U}} + \mathbf{F}_{\text{int}}\mathrm{d}t = \mathbf{F}_{\text{ext}}\mathrm{d}t + \mathrm{d}\mathbf{I} \\ \mathrm{d}\mathbf{I} = \mathbf{L}^{\mathrm{T}}\mathrm{d}\boldsymbol{\lambda}\ ;\ (\mathbf{L}^{\mathbf{T}} = \boldsymbol{\nabla}\mathbf{g}_{\mathbf{N}}) \\ \quad \begin{cases} \dot{\mathbf{g}}_{\mathrm{N}}^{\mathrm{k}} \geq 0 \\ \boldsymbol{\lambda}_{\mathrm{k}} \leq 0 \\ \dot{\mathbf{g}}_{\mathrm{N}}^{\mathrm{k}}.\boldsymbol{\lambda}_{\mathrm{k}} = 0 \end{cases} \end{cases} \quad (2)$$

where k denotes one contact on Γ_C, $\boldsymbol{\lambda}$ is the Lagrange multipliers vectors representing the contact/impact impulses, $\mathbf{M}$ is the mass matrix, $\mathbf{F}_{\text{int}}$ and $\mathbf{F}_{\text{ext}}$ are the internal and the external forces, and $\mathbf{U}$ and $\dot{\mathbf{U}}$ are the semi-discretized displacement and velocity fields, respectively.

Inspired by the well-known Central Difference time-integrator (CD), we present a time-discretization based on an original explicit approach for nonsmooth dynamics with

Lagrange multipliers. Then, the new explicit time integrator with a Lagrange multipliers formulation, over the time step $[t_{n+1/2}, t_{n+3/2}]$ of length Δt, for a contact/impact problem can be summarized as:

$$\begin{cases} \mathbf{M}_{\text{lump}}\left(\dot{\mathbf{U}}_{n+\frac{3}{2}} - \dot{\mathbf{U}}_{n+\frac{1}{2}}\right) = (\mathbf{F}_{\text{ext}} - \mathbf{F}_{\text{int}})\,\Delta t + \mathbf{I}_{n+1} \\ \mathbf{U}_{n+1} = \mathbf{U}_n + \Delta t \dot{\mathbf{U}}_{n+\frac{1}{2}} \\ \mathbf{v}_{n+\frac{3}{2}} = \mathbf{L}_{n+1}\dot{\mathbf{U}}_{n+\frac{3}{2}} \\ \begin{cases} \mathbf{v}^k_{n+\frac{3}{2}} \geq 0 \\ \boldsymbol{\lambda}^k_{n+\frac{3}{2}} \leq 0 \\ \mathbf{v}^k_{n+\frac{3}{2}}.\boldsymbol{\lambda}^k_{n+\frac{3}{2}} = 0 \end{cases} \end{cases} \quad (3)$$

In the following, this time-integrator is called the CD-Lagrange algorithm.

C. Numerical Simulations

In order to test the accuracy and the efficiency of the proposed contact/impact time-integrator (3), some academic examples of dynamic contact/impact problems have been examined.

We present here the well-known bouncing ball example. It is a typical problem in the field of the contact dynamics [2]-[4], involving a ball with a mass m and an initial velocity v_0 (in our case v_0=0), which falls from an initial height z_0. The configuration is depicted in Fig. 1.

The ball hits the ground and lifts off again if the contact is partly elastic or stops if the contact is perfectly plastic. The first case is called Zeno phenomenon where bouncing and free flights alternate infinitely over a finite time interval [0, T].

In Figs. 2 and 3, analytical position and velocity of the ball is compared to the numerical results computed by the CD-Lagrange time-integrator for a coefficient of restitution (dissipated energy occurring in the impact) e=0.8.

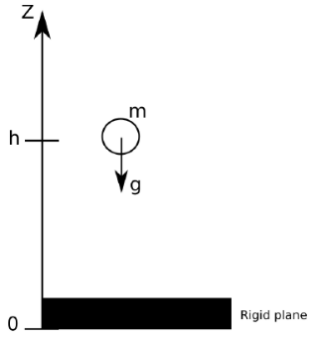

Fig. 1 Configuration of bouncing ball example

The numerical results are found very accurate in predicting the position, the velocity and the downtime of the ball. The algorithm is able to reproduce the Zeno phenomenon, and therefore it belongs to the family of event-capturing methods. In the next step, we use the CD-Lagrange time-integrator to solve contact/impact problem.

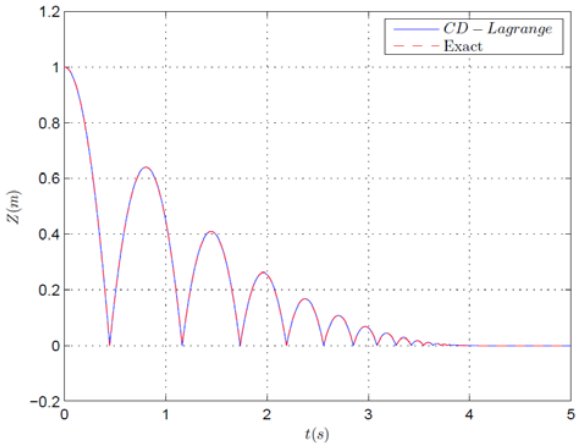

Fig. 2 Analytical and numerical position of the ball

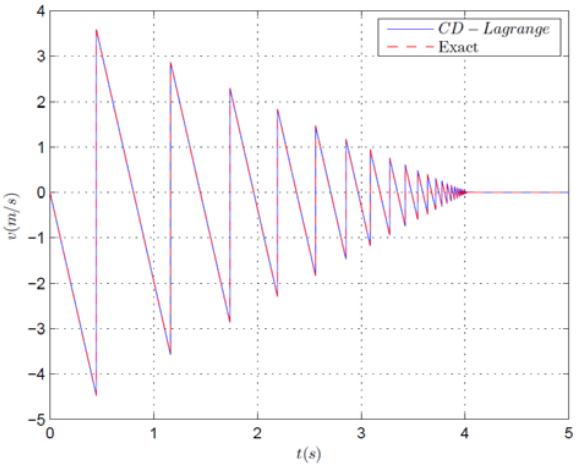

Fig. 3 Analytical and numerical velocity of the ball

III. An Asynchronous Heterogeneous Time Integrator for Contact/Impact Problem

A. Governing Equations

Because of the impacts to which a bridge crane is exposed during a severe earthquake, several time scales coexist. Therefore, a multi-scale strategy needs to be adopted. This method allows an adapted time scale to be selected within the subdomain under consideration with better CPU efficiency compared to standard direct monotime step time-integrators. Consequently, in order to take the high frequency characteristics of impacts into account, we use an explicit temporal scheme in the contact areas. An implicit temporal scheme with greater time steps is adopted for the rest of the structure during the seismic excitations.

The coupling is ensured by a heterogeneous asynchronous time-integrators (HATI). Among those coupling methods, we have applied the method of decomposition into subdomains introduced by [5] and [6]. This approach allows dividing the computation domain Ω in two sub-domains (see Fig. 4). The first sub-domain Ω_E contains the contact areas where the CD-Lagrange time-integrator given in (3) with a suitable mesh is

used. The second sub-domain Ω_I includes the rest of the structure where the implicit Newmark average acceleration scheme is adopted.

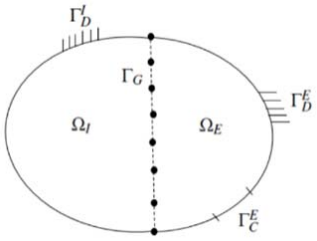

Fig. 4 Configuration of sub-domains

Γ_D^E and Γ_D^I are interfaces on which the displacement is imposed, and Γ_G is the coupling interface between both subdomains. Γ_C^E is the interface of the explicit subdomain where the contact occurs. Let "j" be the micro-time scale, corresponding to time step Δt of explicit scheme (fine time step), and let "m" be the macro-time scale, corresponding to time step ΔT of the implicit scheme (coarse time step), where:

$$\frac{\Delta T}{\Delta t} = m \tag{4}$$

and

$$0 \le j \le m \tag{5}$$

The corresponding equations of the coupling problem, discretized in time and in space, are:

– Balance equations on Ω_I:

$$\mathbf{M}^I \ddot{\mathbf{U}}^I_{n+m} + \mathbf{F}^I_{int,n+m} = \mathbf{F}^I_{ext,n+m} + \left(\mathbf{L}^I_D\right)^T \mathbf{\Lambda}^I_{D,n+m} + \left(\mathbf{L}^I_G\right)^T \mathbf{\Lambda}_{G,n+m} \tag{6}$$

– Balance equations on Ω_E:

$$\mathbf{M}^E \left(\dot{\mathbf{U}}^E_{n+j+\frac{1}{2}} - \dot{\mathbf{U}}^E_{n+j-\frac{1}{2}}\right) + \Delta t\, \mathbf{F}^E_{int,n+j} = \Delta t \left(\mathbf{F}^E_{ext,n+j} + \left(\mathbf{L}^E_D\right)^T \mathbf{\Lambda}^E_{D,n+j} + \left(\mathbf{L}^E_G\right)^T \mathbf{\Lambda}_{G,n+j}\right) + \left(\mathbf{L}^E_C\right)^T \mathbf{\Lambda}_{C,n+j+\frac{1}{2}} \tag{7}$$

– Velocity continuity at Γ_G:

$$\mathbf{L}^E_G \dot{\mathbf{U}}^E_{n+j} + \mathbf{L}^I_G \dot{\mathbf{U}}^I_{n+j} = 0 \tag{8}$$

– Dirichlet boundary conditions on each subdomain:

$$\begin{cases} \mathbf{L}^E_D \dot{\mathbf{U}}^E_{n+j} = 0; & \text{at } \Gamma^E_D \\ \mathbf{L}^I_D \dot{\mathbf{U}}^I_{n+m} = 0; & \text{at } \Gamma^I_D \end{cases} \tag{9}$$

– Unilateral contact conditions at the micro-time step:

$$\begin{cases} \mathbf{v}^k_{n+j+\frac{1}{2}} \ge 0 \\ \mathbf{\Lambda}^k_{C,n+j+\frac{1}{2}} \le 0 \\ \mathbf{v}^k_{n+j+\frac{1}{2}} . \mathbf{\Lambda}^k_{C,n+j+\frac{1}{2}} = 0 \end{cases} \tag{10}$$

Exponent E represents the values linked to the explicit subdomain and exponent I represents those of the implicit one. $\mathbf{L}^i_G$, $\mathbf{L}^i_C$, $\mathbf{L}^i_D$; i = E, I are the matrices respectively corresponding to the relations at the interface Γ_G, the contact condition at interface Γ_C and the Dirichlet conditions on $\mathbf{\Lambda}^i_D$. $\mathbf{\Lambda}^i_j$; j = D, C, G are the Lagrange multipliers matrices.

In the clause B, an industrial example is carried out using the asynchronous contact algorithm described in (6)-(10). This numerical example consists of a bridge crane subjected to a temporal acceleration.

B. Industrial Example: Bridge Crane Under Seismic Loading

An example of a double girder bridge crane is represented on Fig. 5. Its main structure is composed of two girders, two end-carriages and a trolley.

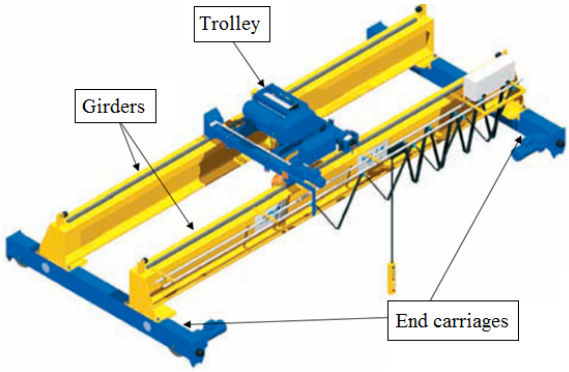

Fig. 5 Example of a double girders bridge crane

A bridge crane operation is characterized by three main motions: the trolley (cross travel) motion on the girders, the long travel motion of the crane on the runway rails and the hoisting motion of the lifted load, driven by the hoist installed on the trolley.

The structures of bridge crane are frequently modelled with beam elements, due to the slenderness of the structure components. Fig. 6 shows the model, where the potential contact areas used for this numerical simulation are identified. This model uses linear elastic beam elements. The decomposition of explicit and implicit sub-domains is depicted in Fig. 7.

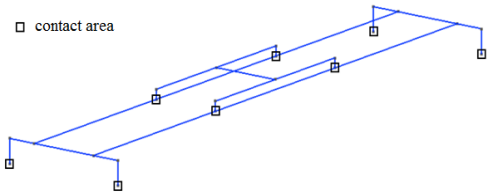

Fig. 6 Bridge crane model using beam elements

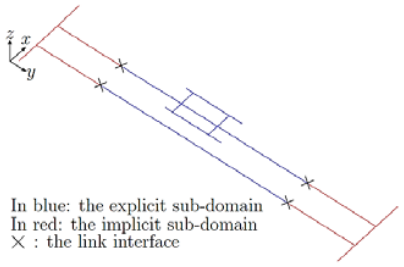

Fig. 7 Bridge crane sub-domains decomposition

The bridge crane is subjected to the gravity. The girders and the end-carriages are subjected to the temporal acceleration, depicted in Fig. 8 along the (-Z) direction.

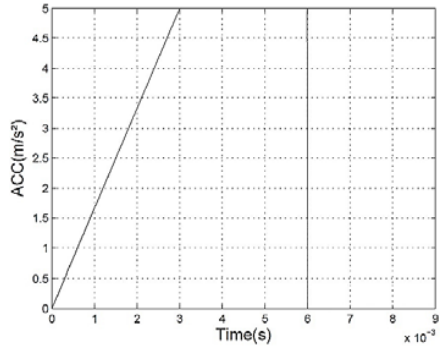

Fig. 7 Acceleration applied to the girders and to the end-carriages in the (-Z) direction

Fig. 8 shows the displacement in the Z direction of one of the four contacts between the trolley and the girders (the same observations can be made for the other contacts). In order to compare a full-explicit method with the explicit-implicit approach developed before, Fig. 9 is a zoom of the displacement for a full-explicit time-integrator (on the left) and an implicit-explicit time-integrator (on the right).

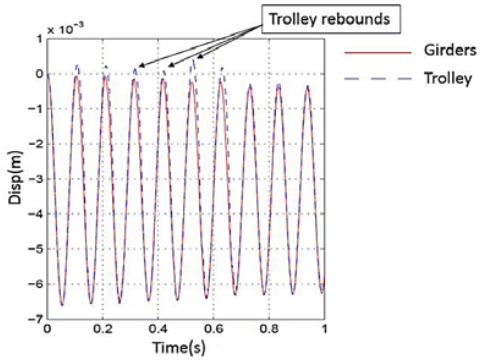

Fig. 8 Acceleration applied to the girders and to the end-carriages in the (-Z) direction

In Fig. 9, we observe that the persistent contact duration and the contact's release time are the same for both methods. This comparison shows that the full-explicit method and the implicit-explicit method give similar results but with the implicit-explicit method showing a significant reduction in CPU time.

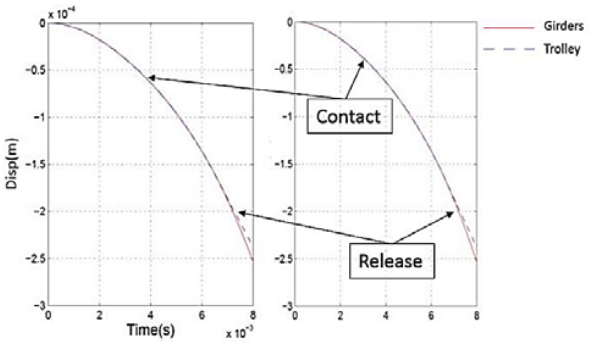

Fig. 9 (a) Full-explicit and (b) implicit-explicit displacement in the Z direction of a contact point

IV. Conclusion

This work has led to the development of a Lagrange explicit event-capturing contact/impact algorithm. The main advantages of this method are that no detection of events is needed, no iterations are used to solve the contact constraints and no additional numerical parameters are to be chosen by the user due to the use of the Lagrange multiplier method.

Time-history dynamic analysis with a multi-scale approach allows accurate numerical resolution. Each subdomain can have its own temporal integrator (heterogeneous) and its own time scale (asynchronous) (see [5]).

The development of such algorithm will make it possible in a second step to gain significantly CPU time in the three-dimensional modelling of bridge cranes subjected to earthquakes.

Acknowledgment

We are grateful to all the colleagues of Cetim and INSA de Lyon, LaMCoS for their contributions and to the French crane manufacturers for great technical support.

References

[1] T. Belytschko, M. Neal, Contact-impact by the pinball algorithm with penalty and lagrangian methods, IJNME 31 (1991) 547-572.
[2] V. Acary, Higher order event capturing time-stepping schemes for nonsmooth multibody systems with unilateral constraints and impacts, Applied Numerical Mathematics 62 (10) (2012) 1259-1275.
[3] B. Brogliato, A. Ten Dam, L. Paoli, F. Genot, M. Abadie, Numerical simulation of finite dimensional multibody nonsmooth mechanical systems, Applied Mechanics Reviews 55 (2) (2002) 107-150.
[4] V. Acary, Projected event-capturing time-stepping schemes for nonsmooth mechanical systems with unilateral contact and coulombs friction, Computer Methods in Applied Mechanics and Engineering 256 (2013) 224-250.
[5] A. Gravouil, A. Combescure, A multi-time-step explicit-implicit method for non-linear structural dynamics, IJNME, 50, pp. 199-225, 2001.
[6] A. Gravouil, A. Combescure, M. Brun, Heterogeneous asynchronous time integrators for computational structural dynamics, IJNME, accepted, 2014.